

Investigation of Temperature effects for a finite elasto-hydrodynamic journal bearing lubricated by Ferro fluids with couple stresses

Kihuga Daniel¹, Kinyanjui Mathew² and Kimathi Mark³

Abstract

The performance of finite elasto-hydrodynamic journal bearings lubricated by ferrofluids with couple stresses has been studied. We derive the energy equation that takes into account magneto elasto-hydrodynamics. The energy equation obtained is solved numerically by the finite difference technique since it is highly non-linear. The numerical scheme used is implemented in MATLAB so as to obtain the approximate solutions. The temperature distributions are obtained and the solutions obtained represented in graphs. It is clear from the results that the temperature increases with the increase in magnetism and the couple stress. The prandtl number, Erkert number and the bearing length increase the bearing temperature. The results can be used to improve the bearing performance in the engineering field.

¹ Jomo Kenyatta University of Agriculture and Technology.

E-mail: kihugadaniel36@gmail.com

² Jomo Kenyatta University of Agriculture and Technology.

E-mail: mathewkiny@yahoo.com

³ Technical University of Kenya. E-mail: memkimathi@gmail.com

Keywords: Couple stresses; Elasto-hydrodynamic; Journal bearing; Temperature distributions

1 Introduction

A bearing is a system of machine elements whose function is to support an applied load by reducing friction between the relatively moving surfaces. Journal bearing is subset of bearings used to support rotating shafts that use the principle of hydrodynamic lubrication. The journal bearing is made up of four main parts as in the Figure 1. This type of bearings is one of the most common forms and is used in a wide variety of machines. When designing such lubricating system, the heat, and load and flow rate required for a bearing must be known to properly size the lubricating oil pumps, coolers among other bearing machines. Bearing type and size are based on rotor weight, rotor rotations per minute (RPM), and lubricant characteristics Govindaraj *etal* (2012). The characteristics of hydrodynamic journal bearing have been the subject of many researches. Some being directed to the bearing geometry design and others devoted to the study of the lubricant properties. The recent solutions (Nada & Osman, 2007) that have encouraged the study of the lubricant properties have been used with other parameters being considered in predicting the journal bearing behavior. These behaviors such as the load carrying capacity, type of lubricant flow region (laminar or turbulent flow), type of lubricant (Newtonian or non-Newtonian), inertia and acceleration effects, and magnetic effect in the case of using ferrofluid (Nada, 2002).

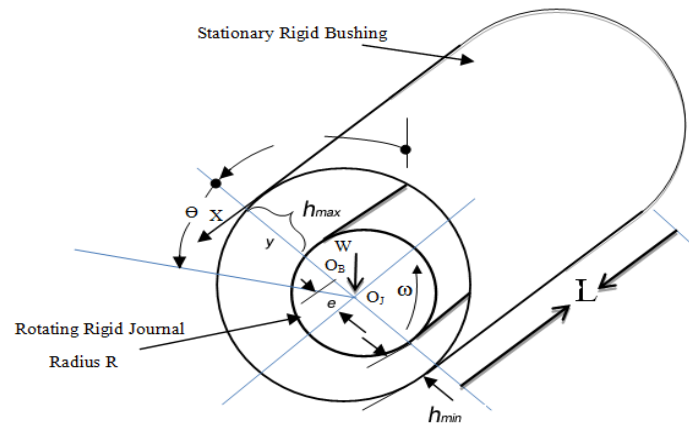


Figure 1: Scheme of the examined bearing

Although many aspects of bearing performance are fully solved, there is still need for further investigations on how to improve the bearing performance and its characteristics.

2 Literature Review

Wear is the major cause of material wastage and loss of mechanical performance of machine elements, and any reduction in wear can result in considerable savings which can be made by improved friction control. Lubrication is an effective means of controlling wear and reducing friction, and it has wide applications in the operation of machine elements such as bearings. The principles of hydrodynamic lubrication were first established by a well-known scientist Osborne Reynolds in 1886 and he explained the mechanism of hydrodynamic lubrication through the generation of a viscous liquid film between the moving surfaces.

The journal bearing design parameter such as load capacity can be determined from Reynolds equation both analytically and numerically (Hamrock, 1994). Saynatjoki and Holmberg (1982) described a magnetic fluid as not a simple fluid; it is a stable suspension of small particles of ferromagnetic materials in a base fluid.

For the purpose of ensuring the colloid stability, a surfactant of polymers (such as oleic acid) is usually introduced into the suspension. This will create around each single particle a coating layer to prevent the agglomeration of the particles by the magnetic field effect or by the molecular attraction. When a magnetic field is applied to the magnetic fluid, each particle experiences a force that depends on the magnetization of the magnetic material of the particles and on the strength of the applied field.

Investigation on the lubrication of lightly loaded cylinders in combined rolling, sliding, and normal motion with a couple stress fluids as lubricant under cavitation boundary conditions was done by Bujurke and Naduvinamani (1990). They noted that the load capacity and the frictional drag increased as the squeeze velocity increased. Increasing the couple stress parameter enhanced this increase. Presentation on the study of performance of finite journal bearings lubricated with a fluid with couple stresses taking into account the elastic deformation of the liner have been done by Mokhiamer *et al* (1999). They concluded that the influence of couple stresses on the bearing characteristics was significantly apparent.

Study on the static characteristics of rotor bearing systems lubricated with couple stress fluids with the effect of surface roughness considerations have been done clearly by Naduvinamani *et al* (2002) and Naduvinamani *et al* (2002). They formulated and solved for transverse and longitudinal roughness for these problem. Nada and Osman (2007) investigated the static performance of finite hydrodynamic journal bearings lubricated by magnetic fluids with couple stresses and among their conclusion was that the magnetic lubricant gives higher load carrying capacity, higher attitude angle, lower friction coefficient, and higher side leakage. These effects are more significant where the hydrodynamic effects are low, at the lower values of couple stress parameter and eccentricity ratios.

Thermal effects on hydrodynamic journal bearings lubricated by magnetic fluids and with couple stresses were studied by Abdo *et al* (2009). They concluded that the magnetic lubrication gives higher pressure distribution, with small

insignificant fluid temperature rise. The load carrying capacity increases without increase of the friction force. They also found that the magnetic lubrication has decreased the effect of the side leakage such that the bearing may operate without any side leakage. Taking into account of the couple force their results shown that lubricants with couple stresses compared with Newtonian lubricants increase the pressure and temperature especially at high eccentricity ratios. The couple stresses give increase in both load carrying capacity and friction force and decrease in friction coefficient. Thus it can be concluded that fluids with couple stresses are better than Newtonian fluids.

Priyanka *et al*, 2012 reviewed the analysis of hydrodynamic journal bearing and in their work they presented a survey of important papers pertaining to analysis of various types of methods, equations and theories used for the determination of load carrying capacity, minimum oil film thickness, friction loss, and temperature distribution of hydrodynamic journal bearing. Predictions of these parameters are the very important aspects in the design of hydrodynamic journal bearings. They focused on various types of factors which tremendously affect the performance of hydrodynamic journal bearing. They found that friction coefficient is increased, with increasing wear depth as well as misalignment and Sommerfeld number. The friction coefficient and consequently the power loss are strongly dependent upon the misalignment angle and wear depth. The noise of the bearing decreases as the mass eccentricity of the rotor decreases, the lubricant viscosity increases, the width of the bearing increases, and the radial clearance of the bearing decreases.

Daniel and Calvalca, 2013 evaluated the thermal effects in tilting pad bearing where their results showed that the temperature increases as the rotational speed increases due to the shear rate of the oil film. The maximum temperature in the bearing occurred in the overloaded pad, near the outlet boundary. They performed experimental tests in a tilting pad journal bearing operating in a steam turbine to validate the model. Comparing the experimental and numerical results they provided a good correlation. They finally concluded that the thermo-hydrodynamic lubrication

as developed in their work is promising to consistently evaluate the behavior of the tilting pad journal bearing operating in relatively high rotational speeds.

Nessil *et al*, 2012 did an analysis of journal bearings lubrication using non-Newtonian fluids which they described by a power-law model. They determined the performance characteristics of the journal bearings for various values of the non-Newtonian power-law index “ n ”. The numerical results they obtained showed that for the dilatant fluids ($n > 1$), the load-carrying capacity, the pressure, the temperature, and the frictional force increased while for the pseudo-plastic fluids ($n < 1$) they decreased. Thermo-hydrodynamic analysis of a Journal bearing using CFD as a tool was done by Muhesh *et al*, 2012. From the results they obtained, it was clear that temperature created from the frictional force increase as the viscosity of the lubricant decrease and lesser viscosity decreases the maximum pressure of the lubricant inside the bearing.

3 Problem Modeling

Considering the equation of energy of hydro magnetic flows below

$$\rho C_v \frac{DT}{Dt} = k \nabla^2 T + \mu \phi + \frac{1}{\sigma} J^2 \quad (3.1)$$

The energy equation is changed due to electric dissipation which is the heat energy produced by the work done by electric current. The electric dissipation is referred to as the joule’s heating and is given as $\frac{1}{\sigma} J^2$. The term $\mu \phi$ is the internal heating due to viscous dissipation. For an incompressible fluid flow, viscous dissipation function ϕ in three dimensions is expressed as;

$$\begin{aligned} \varphi = 2 & \left[\left(\frac{\partial u}{\partial x} \right)^2 + \left(\frac{\partial v}{\partial y} \right)^2 + \left(\frac{\partial w}{\partial z} \right)^2 \right] + \left[\left(\frac{\partial u}{\partial y} + \frac{\partial v}{\partial x} \right)^2 + \left(\frac{\partial v}{\partial z} + \frac{\partial w}{\partial y} \right)^2 + \left(\frac{\partial w}{\partial x} + \frac{\partial u}{\partial z} \right)^2 \right] \\ & - \frac{2}{3} \left(\frac{\partial u}{\partial x} + \frac{\partial v}{\partial y} + \frac{\partial w}{\partial z} \right)^2 \end{aligned} \quad (3.2)$$

The term $\left(\frac{\partial u}{\partial x} + \frac{\partial v}{\partial y} + \frac{\partial w}{\partial z} \right)$ reduces to zero since it represents the equation of continuity. The partial derivatives of v ; such as $\frac{\partial v}{\partial x}$, $\frac{\partial v}{\partial y}$ and $\frac{\partial v}{\partial z}$ vanishes since all are equal to zero. The bearing is parallel to the x-axis, and therefore the contribution of the terms $\frac{\partial u}{\partial x}$ and $\frac{\partial w}{\partial x}$ to viscous dissipation is assumed to be negligible and the terms are therefore dropped from the equation. Also, the z-axis is infinite and thus the partial derivatives with respect to z are dropped from the equation. Therefore, the viscous dissipation equation reduces to;

$$\varphi = 2 \left[\left(\frac{\partial u}{\partial y} \right)^2 + \left(\frac{\partial w}{\partial y} \right)^2 \right] \quad (3.3)$$

Considering the use of the Electromagnetic equations as the Maxwell's equations as discussed below;

3.1 Maxwell's equations

The Maxwell's equations give the relation between the interacting electric and magnetic fields. Maxwell's equations consist of four fundamental electromagnetic equations for time varying magnetic field and these equations are given as below;

$$\nabla \times E = -\frac{\partial B}{\partial t} \quad \text{Or} \quad \nabla \times E = \mu \frac{\partial H}{\partial t} \quad (3.4)$$

$$\nabla \times H = J + \frac{\partial D}{\partial t} \quad (3.5)$$

$$\nabla \cdot \mathbf{D} = \rho_e \quad (3.6)$$

$$\nabla \cdot \mathbf{B} = 0 \quad (3.7)$$

Equation (3.4) is the Faraday's law that was named after Michael Faraday, who in 1831, experimentally discovered that a current is induced in a conducting loop when magnetic flux linking the loop changes. It is an experimental law and can be considered as an axiom (truth without proof). This equation expresses an axiom (statement taken true without proof) for electromagnetic induction which means that the electric field intensity in a region of time varying magnetic flux density is non-conservative and cannot be expressed as a gradient or scalar potential.

Equation (3.5) is the Ampere's law that was named after Ampere Andre-Marie, and which states that wires carrying electric currents attract and repel each other magnetically.

From Maxwell's electromagnetic equations, the relation $\nabla \cdot \mathbf{B} = 0$ yields $\frac{\partial B}{\partial y} = 0$. When the magnetic Reynolds number is small, induced magnetic field is negligible in comparison with the applied magnetic field. This therefore leads to;

$$B_x = B_z = 0 \quad \text{and that} \quad B_y = B_0 \quad (\text{a constant})$$

The current density \mathbf{J} has the components (J_x, J_y, J_z) . Therefore, the equation of conservation of electric charge $\nabla \cdot \mathbf{J} = 0$ where it gives that;

$$J_y = \text{a constant}$$

Since the bearing wall is non-conducting, $J_y = 0$ at the bearing wall and hence it becomes zero everywhere in the flow. Neglecting the polarization effect, the electric field $\mathbf{E} = 0$. Therefore giving

$$\mathbf{J} = (J_x, 0, J_z), \quad \mathbf{B} = (0, B_0, 0) \quad \text{and} \quad \mathbf{q} = (u, v, w) \quad (3.8)$$

The general Ohms law is expressed as;

$$\mathbf{J} = \sigma(\mathbf{E} + \mathbf{q} \times \mathbf{B}) \quad (3.9)$$

The magnetic field is considered to act only from one direction (divergence less).

This means that there are no magnetic flux sources and sinks within the field, and therefore $\nabla \cdot B = 0$. The mathematical expression of the continuity equation in the case of conservation of electric charge becomes;

$$\nabla \cdot J = -\frac{\partial \rho_e}{\partial t} \quad (3.10)$$

The term $q \times B$ in equation (3.9) thus yields

$$q \times B = \begin{vmatrix} i & j & k \\ u & v & w \\ 0 & B_0 & 0 \end{vmatrix} = -wB_0i + uB_0k \quad (3.11)$$

Therefore, from equations (3.9) and (3.11), the x-axis and z-axis components of the current density respectively become;

$$J_x = -\sigma wB_0 \quad \text{and} \quad J_z = \sigma uB_0 \quad (3.12)$$

Now, the Lorentz force $J \times B$ becomes;

$$J \times B = \begin{vmatrix} i & j & k \\ -\sigma wB_0 & 0 & \sigma uB_0 \\ 0 & B_0 & 0 \end{vmatrix} = -\sigma uB_0^2i - \sigma wB_0^2k \quad (3.13)$$

Heat generated due to electrical resistance of the fluid to the flow of the induced electric current is given as the joule heating which yields;

$$\frac{J^2}{\sigma} = \sigma w^2B_0^2 + \sigma u^2B_0^2 = \sigma B_0^2(u^2 + w^2) \quad (3.14)$$

Taking viscous dissipation (3.3) and the joules heating (3.14) into considerations the equation of energy becomes.

$$\begin{aligned} \rho C_p \left(\frac{\partial T}{\partial t} + u \frac{\partial T}{\partial x} + w \frac{\partial T}{\partial z} \right) = \\ = k \left(\frac{\partial^2 T}{\partial x^2} + \frac{\partial^2 T}{\partial z^2} \right) + 2\mu \left[\left(\frac{\partial u}{\partial y} \right)^2 + \left(\frac{\partial w}{\partial y} \right)^2 \right] + \sigma B_0^2 (u^2 + w^2) \end{aligned} \quad (3.15)$$

4 Non-dimensionalization

The subject of dimensional analysis considers how to determine the required set of scales for any given problem. This is a process that starts with selecting a suitable scale against which all dimensions in a given physical model are scaled. This process aims at ensuring that the results obtained are applicable to other geometrically similar configurations under similar set of flow conditions. The non-dimensional parameters used are defined as below:

$$x = R\theta \quad y = Cy^* \quad z = L_b Z \quad t = \frac{Ht^*}{U_\infty} \quad T = T^*(T_w - T_\infty) + T_\infty \quad u = u^*U_\infty \quad w = w^*U_\infty$$

Using these non-dimensional parameters above, the specific energy equation (3.15) becomes;

$$\left(\frac{1}{C} \frac{\partial T^*}{\partial t^*} + \frac{u^*}{R} \frac{\partial T^*}{\partial \theta} + \frac{w^*}{L_b} \frac{\partial T^*}{\partial Z} \right) = \frac{k}{\rho C_p U_\infty} \left(\frac{1}{R^2} \frac{\partial^2 T^*}{\partial \theta^2} + \frac{1}{L_b^2} \frac{\partial^2 T^*}{\partial Z^2} \right) + 2\mu \frac{U_\infty}{\rho C_p (T_w - T_\infty) C^2} \left[\left(\frac{\partial u^*}{\partial y^*} \right)^2 + \left(\frac{\partial w^*}{\partial y^*} \right)^2 \right] + \frac{\sigma B_0^2 U_\infty}{\rho C_p (T_w - T_\infty)} (u^{*2} + w^{*2}) \quad (3.16)$$

5 Finite difference Technique

5.1 Introduction

The performance of the bearing in this study has been predicted assuming adiabatic conditions with magnetic fluid lubricant with couple stress. The effect of magnetic force coefficient, couple stress parameter and length to diameter ratio and temperature distribution has been numerically investigated.

5.2 The Specific Energy Equation in Finite Difference

Considering the specific non-dimensional energy equation (3.16) and applying the finite difference technique, using the central difference method, the specific

energy equation in finite difference becomes;

$$2T_{(i,j)}^* = \left\{ \frac{L_b^2 (\Delta Z)^2 (T_{(i+1,j)}^* + T_{(i-1,j)}^*) + R^2 (\Delta \theta)^2 (T_{(i,j+1)}^* + T_{(i,j-1)}^*)}{L_b^2 (\Delta Z)^2 + R^2 (\Delta \theta)^2} \right\} - \left(\frac{\rho C_p U_\infty}{K} \right) \frac{RL_b (\Delta \theta) (\Delta Z)}{L_b^2 (\Delta Z)^2 + R^2 (\Delta \theta)^2} \times \left[\frac{L_b (\Delta Z) u^* (T_{(i+1,j)}^* - T_{(i-1,j)}^*) + R (\Delta \theta) w^* (T_{(i,j+1)}^* - T_{(i,j-1)}^*)}{2} \right] \quad (3.17)$$

This final equation is thus solved using a computer code in MATLAB application software.

6 Results and Discussions

The journal bearing used is as in the Figure 1. It has two components, one representing the shaft and the other the bearing. The system is supplied by lubricant fluid through openings which emerge in an axial groove. The results simulate the temperature profiles and how the parameters such as the magnetic parameter, couple stress parameter and the eccentricity ratio affects the bearing temperature and the performance of the bearing. The results are discussed herein:

Figure 6.1 shows the Non-dimensional temperature distribution (T) for constant eccentricity ratio applying some magnetic force and for length to diameter ratio 1.0 across the bearing ends. This figure displays temperature distributions over the whole bearing at the same eccentricity ratio applying magnetic force, $\alpha = 0.8$ and the couple stress parameter $L = 0.2$. The surface as seen in the figure 6.1 clearly shows the temperature distributions with the bearing length and theta θ . It is found that the temperature increases slightly in the region $\theta = 0.0$ to $\theta = 0.5\pi$ after that the rate increases rapidly within the region $\theta = 0.5\pi$ to $\theta = 1.5\pi$, then rate of increase of temperature in the region $\theta = 1.5\pi$ to $\theta = 2\pi$ is

approximately considered to be dropping as the fluid goes back to meet with fresh lubricant at insertion point at $\theta = 0.0$. Due to no slip property, lubricant layers slid over each other and thus due to friction the temperature increases

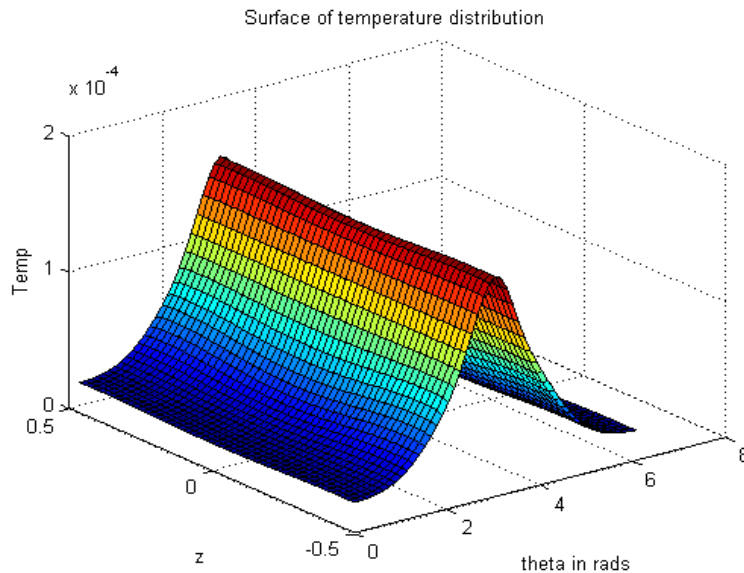


Figure 6.1: plot of surface of Temperature with theta and z at $L = 0.2$

Temperature profile again is shown clearly in the wire frame map Figure 6.2 which shows the 3D Temperature distributions over the whole bearing at the same eccentricity ratio applying magnetic force, $\alpha = 0.8$ and the couple stress parameter $L = 0.5$. It is evident that as the value of couple stress parameter increases, the temperature of the bearing increases as well. This is seen as we compare the non-dimensional maximum temperatures in Figure 6.1 which is approximately 1.5 and that in Figure 6.2 which is approximately 2.5. Therefore, the higher the couple stress parameter L increases so does the bearing temperature.

Considering the Prandtl number effect on the bearing temperature, we vary the value of the Prandtl number to see the effect while holding the factors and parameters a constant. This is evident clearly as from Figure 6.3. There is decrease in temperature as the value of the Prandtl number decreases. Since the Prandtl number is the ration between viscus diffusion and thermal diffusion. Therefore, if

Prandtl number is small, then the heat in the bearing diffuses quickly compared to the velocity. This is physically true from the Figure 6.3 since, as the Prandtl number reduces, so does the temperature in the bearing.

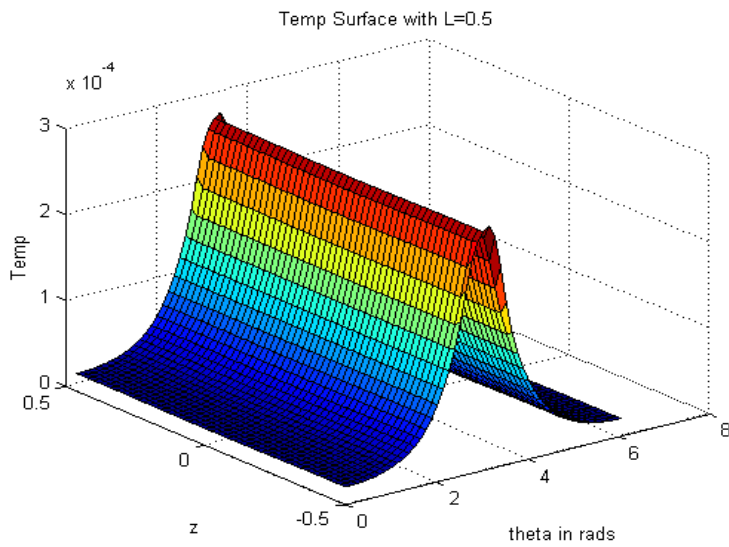


Figure 6.2: plot of surface of Temperature with theta and z at $L = 0.5$

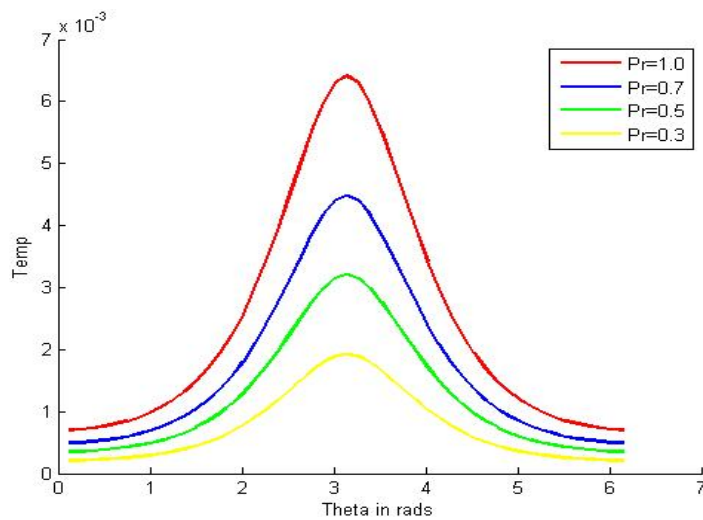


Figure 6.3: Graph of Temperature against theta at different Prandtl Number

Considering the Eckert number effect on the bearing temperature, we vary the value of the Eckert number to see the effect while holding the other factors and parameters a constant. This is evident clearly as from Figure 6.4. There is decrease in temperature as the value of the Eckert number decreases. Geropp's work was focused on high rotational Reynolds numbers, where the frictional heat created by dissipation and thereby the Eckert number, gains influence on the heat transfer and this is also true from this work. The dimensionless Eckert number

$$Ec = \frac{\frac{1}{2}v^2}{C_p(T_w - T_\infty)},$$

therefore plays an important role, representing the ratio of kinetic energy at the wall to the specific enthalpy difference between wall and fluid. Since the Eckert number is the ration between viscous diffusion and thermal diffusion. Therefore, if Eckert number is small, then the heat in the bearing diffuses quickly compared to the velocity. This is physically true from the Figure 6.4 since, as the Eckert number reduces, so does the temperature in the bearing.

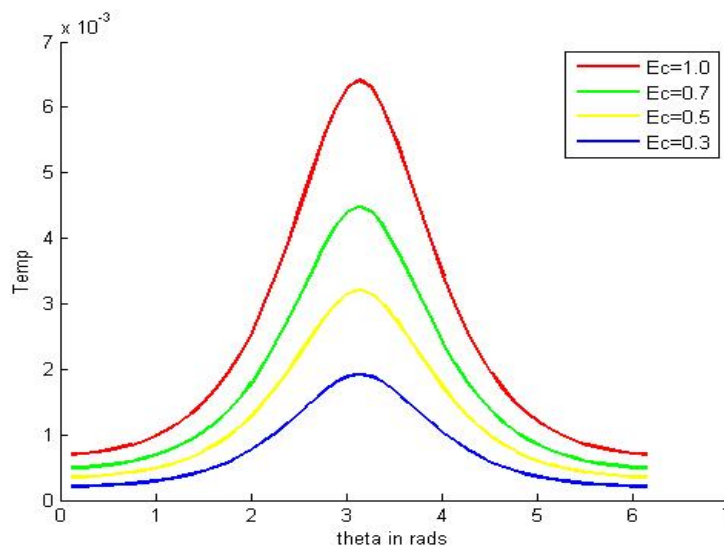


Figure 6.4: Graph of Temperature against theta at different Eckert Number

The Figure 6.5 represents the plot of film thickness against arc length θ with eccentricity ratio ranging from $e = 0.0$ to $e = 0.6$. It is found that as the eccentricity ratio increases so does the film thickness. This effect increases the hydrodynamic effect hence the bearing can carry higher values of the load applied on the bearing. Also the temperature distribution is affected by changing the eccentricity ratio; higher eccentricities are always associated with higher temperature rise. This agrees with that of Monira, 1982. The results indicate that the magnetic lubrication has insignificant effect on the lubricant maximum temperature at all eccentricity ratio. In fact, it is from the good benefit for the magnetic lubricant.

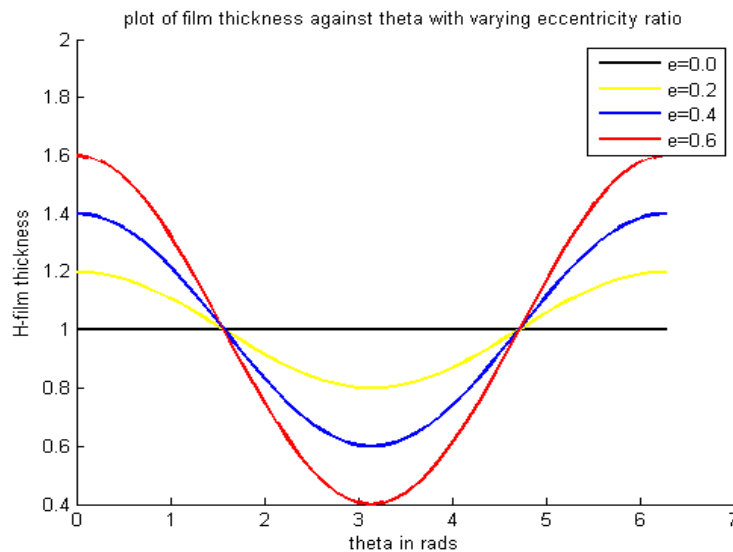


Figure 6.5: Graph of film thickness against theta at different eccentricity ratio values

7 Conclusion

We have considered that the fluid is incompressible in that the density is held constant and that the viscosity coefficient is also constant. From the study, having that there is change in temperature, then the viscosity and density of the fluid should be changing as well. We therefore recommend that an extension in research of the

same elasto-hydrodynamic journal bearing with viscosity and the density being taken as variables be a food for thought for advanced research in this area.

ACKNOWLEDGEMENTS: Thanks Mr. Kihuga Samuel and Mrs. Lucy Kihuga for your support, encouragement and prayers all through this work. God bless you.

References

- [1] Govindaraj R., and Satishkumar V. M., *Design of journal bearing test rig. Sweden: Blekinge Tekniska Hogskola*, 2012.
- [2] Nada, G S, and T A Osman, *Static Performance of Finite Hydrodynamic Journal Bearings Lubricated by Magnetic Fluids with Couple Stresses*, Egypt: Springer Science and Business Media, 2007.
- [3] Nada, G.S., *Static and Dynamic Characteristics of Magnetized Journal Bearings Lubricated with Ferrofluid*, PhD Thesis in Mechanical Engineering, Faculty of Engineering, Cairo, Egypt: Cairo University, 2002.
- [4] Hamrock, B J., *Fundamentals of fluid film lubrication*, New York: New York: McGraw-Hill, 1994.
- [5] Saynatjoki, M, and K Holmberg, *Magnetic fluids in sealing and lubrication—a state of art review*. Finland: Technical Research Center of Finland, 1982.
- [6] Bujurke, N M, and N B Naduvinamani, The lubrication of lightly loaded cylinders in combined rolling, sliding and normal with couple stress fluid, *Int. J.Mech. Sci*, (1990), 969-979.
- [7] Mokhiamer, U M, W A Crosby, and H A El-Gamal, A study of a journal bearing lubricated by fluids with couple stress considering the elasticity of the liner, *Wear*, (1999), 194-201.

- [8] Naduvinamani, N.B, P.S Hiremath, and G. Gurubasavaraj, Effect of surface roughness on the static characteristics of rotor bearings with couple stress fluids, *Comput. Struct*, **80**, (2002), 1243-1253.
- [9] Naduvinamani, N.B, P.S Hiremath, and G Gurubasavaraj, Surface roughness effects in a short porous journal bearing with a couple stress fluid, *Fluid Mech.*, (2002), 333-354.
- [10] Abdo S. H., Osman S. G., Nada G. G. and Abdel-Jaber T. G., *Thermal Effects on Hydrodynamic Journal Bearings Lubricated by magnetic Fluids with Couple Stresses*, Thesis in Mechanical Design and Production Engineering, Cairo University, 2009.
- [11] Priyanka T. and Veerendra K., Analysis of Hydrodynamic Journal bearing- A review, *International Journal*.
- [12] Geropp D: Der turbulente Wärmeübergang am rotierenden Zylinder. *Ingenieur Archiv*, **38**, (1969), 195.
- [13] Cavalca K. L. and Daniel G. B., Evaluation of the thermal effects in tilting pad bearing, *Scientific world Journal*, (2013).
- [14] Nessil A., Salati L., Hacene B. and Muamar M., Journal bearing lubrication Aspect Analysis Using Non-Newtonian Fluids., *Scientific world journal*, (2012).
- [15] Muhesh S., Ashish K. G. and Ashish D. , Thermohydrodynamic analysis of a Journal bearing using CFD as a Tool, *I.J.S.R.*, (2012), 2250-3153.